International Journal of Thermodynamics (IJoT)
ISSN 1301-9724 / e-ISSN 2146-1511
www.ijoticat.com

Vol. 17 (No. 3), pp. 189-198, 2014
doi: 10.5541/ijot.528
Published online: September 01, 2014

The Thermodynamics of Exercise Science*

R. J. Simeoni

School of Allied Health Sciences, Griffith University Gold Coast, Queensland 4222, Australia
E-mail: r.simeoni@griffith.edu.au

Abstract

This article describes the "human body engine" via a thermodynamics-based model that considers the work associated with gas pressure, volume and temperature changes for the glucose-based equation of respiration. The efficacy of the model is supported by prior studies that: accurately predict the slow component of oxygen uptake kinetics; quantitatively explain observed race splitting strategies within endurance events; and accurately predict maximum velocities in endurance swimming. These prior studies are summarized by the review component of the present article which additionally presents new temperature-dependent efficiency implications especially relevant for heat-affected athletes. The new model implications support reported experimental observations and also potentially provide quantified clarity to an area of exercise physiology research known to be challenged by opposing experimental findings, thus providing further support for model efficacy. A 0.32% efficiency decline per 1 ^{o}C increase in core body temperature is predicted. The model is also applied to the "ice slurry ingestion" regime which reportedly offers significant performance advantages (greater than that predicted by the model based on core temperature change alone) for endurance athletes competing in the heat, and the model reconciles with such advantages when ice slurry effect on arterial exchange temperatures and partial pressures are incorporated.

Keywords: *Exercise; oxygen uptake; temperature; thermodynamics.*

1. Aims and Scope

A high volume of research attempting to explain, or provide further insight into, a physiological basis for the slow component of oxygen uptake kinetics has been evident within the present study's host research Department for almost two decades. Indeed, more generally the provision of a complete physiological explanation for this slow component has challenged exercise scientists for an even longer period, with comparison of slow component profiles between various subject groups (e.g., trained versus untrained, endurance event versus anaerobic event) and between different clinical stimuli for similar subject groups (e.g., response comparisons for different training methods), representing just a small cross-section of study types within this field of research [1]–[6].

In recent years it was recognized that a thermodynamics-based explanation, involving a loss in "human body engine" efficiency during exercise, may exist for the slow component. The resulting explanatory model proved accurate in the prediction of key clinical observations, and simply considers the thermodynamical work associated with gas pressure, volume and temperature changes for the glucose-based equation of respiration [7], [8]. Sections 3 and 4 of the present article review conference published works for the model, while Section 5 presents new temperature-based model implications. An introduction to oxygen uptake kinetics is first given in Section 2.

2. Oxygen Uptake Kinetics Introduction

The rate of human oxygen consumption is referred to as oxygen uptake or $\dot{V}_{O_2}$, and is typically expressed in liters per minute. Cycle and treadmill ergometry are examples of typical exercise tests during which $\dot{V}_{O_2}$ profiles are recorded and analyzed within a clinical setting by exercise physiologists, as per the cycle ergometry photograph of Figure 1 for exercise science students at Griffith University.

Figure 1. Oxygen uptake monitoring during cycle ergometry for Griffith University exercise science students.

A typical $\dot{V}_{O_2}$ profile during constant-load high power (severe) exercise is given by Figure 2. The profile in Figure 2 exhibits three distinct phases. Phase 1 is the initial rapid increase from baseline and is said to originate from a blood circulatory delay [5]. Phase 2, also known as the fast or primary phase, reaches $\dot{V}_{O_{2,SS}}$, a hypothetical steady-state asymptote for the remainder of the exercise which is observed in practice for light-to-moderate exercise. Phase 2 is said to be dictated by intramuscular processes and

*This paper includes a review component of papers published in proceedings of the Australian Institute of Physics National Congress: Physics for the Nation 2005, and the International Conference on Bioinformatics and Biomedical Engineering 2011.

*Corresponding Author

changes in body oxygen stores [4]. The final phase 3, referred to as the slow component of oxygen uptake, is a gradual upward trend away from $\dot{V}_{O_2,SS}$, exhibited for high power exercise performed above the lactate threshold. The mechanisms behind phase 3 have captivated and challenged exercise physiologists for decades as previously cited. Some suggested mechanisms involve the progressive recruitment of less efficient fast-twitch muscle fibers; a temperature-induced oxygen cost known as the *Q*10 effect; the oxygen cost of increased ventilation; and metabolism of blood lactate [6].

Phases 2 and 3 are typically modeled by monoexponential equations [9] for which relaxation time constant comparisons between subject groups (e.g., young versus elderly, trained versus untrained) are common within this field of exercise physiology. An example phase 3 equation takes the form $\dot{V}_{O_2}(t) = \dot{V}_{O_2,SS} + \Delta\dot{V}_{O_2,slow}\left(1 - e^{-\lambda t}\right)$, where t is the time from the onset of phase 3, λ is the phase relaxation time constant and $\Delta\dot{V}_{O_2,slow}$ is the absolute change in $\dot{V}_{O_2}$ for the phase. However, it should be noted that phase 3 may also display linear rather than monoexponential behavior [2], [6].

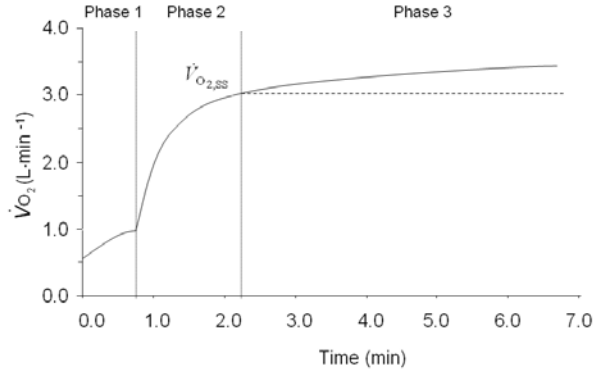

Figure 2. Three phases of oxygen uptake ($\dot{V}_{O_2}$) for constant-load high power exercise. $\dot{V}_{O_2,SS}$ represents a hypothetical steady-state that is characteristic in practice for light exercise.

Initial precursory research [7] to the present study showed that the slow component can be explained from a rudimentary thermodynamics perspective that considers the work associated with gas pressure, volume and temperature changes for the glucose-based equation of respiration. That initial research is reviewed directly below.

3. Review of Slow Component Thermodynamic Modeling

3.1 Thermodynamic Model Background

Work is performed by a gas as it expands. The work is quantified as the area under a pressure, *P*, versus volume, *V*, graph for the gas as it undergoes this expansion, which may or may not be isothermal or adiabatic in nature. Air contains O_2 (21%) and CO_2 (<0.1%), leading to partial pressures of p_{O_2} = 152 mm Hg and p_{CO_2} = 0.3 mm Hg. For inhaled air, alveolar and arterial p_{O_2} are both approximately 105 mm Hg and O_2 exists at a core body temperature of $T_{core} \approx 37.0$ °C. When glucose is utilized as an energy source, one mole of CO_2 is produced for every mole of O_2 in accordance with the chemical equation, $C_6H_{12}O_6 + 6O_2 \rightarrow 6CO_2 + 6H_2O + energy$, of respiration. Thus, from a purely mechanical perspective the work performed by the "human body engine" may be depicted as the work of gas expansion for a one-step process from initial arterial to final atmospheric gaseous conditions (whereby arterial O_2 is ultimately converted into CO_2 expelled to atmospheric conditions), as depicted by the one-step flow diagram of Figure 3. Note that the term human body engine is indeed appropriate since an engine can generally be defined as a system in which the chemical potential energy of a fuel is transferred to mechanical energy or work, with the fuel burning in oxygen to produce a larger volume of hot gas, the expansion of which brings about system energy transfer.

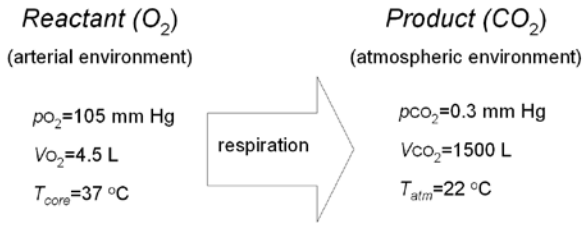

Figure 3. Environmental conditions for the gaseous reactant and product of respiration, considered as a one-step process from artery to atmosphere for an exercise duration of 1 minute. Note that V_{O_2} = 4.5 L (arterial) corresponds to V_{O_2} = 3.0 L (atmospheric).

The choice of V_{O_2} = 4.5 L as the arterial volume of O_2 in Figure 3 is based on a $\dot{V}_{O_2}$ of 3.0 L·min^{-1} recalculated from atmospheric to arterial conditions using the ideal gas law, for an exercise duration of 1 minute. The expelled volume of CO_2, V_{CO_2} in Figure 3, is also derived from the ideal gas law, i.e., $V_{CO_2} = p_{O_2} \cdot V_{O_2} \cdot T_{atm} / (T_{core} \cdot p_{CO_2})$, where T_{atm} is atmospheric temperature.

The area under the reactant-to-product *P*-*V* graph for the above respiration equation represents the work, *W*, performed by the body engine, and application of a trapezoidal area approximation gives $W = (V_{CO_2} - V_{O_2})(p_{O_2} + p_{CO_2})/2$. Substitution of the previously derived expression for V_{CO_2} then gives

$$W = (p_{O_2} \cdot V_{O_2} \cdot T_{atm} / [T_{core} \cdot p_{CO_2}] - V_{O_2})(p_{O_2} + p_{CO_2})/2 \quad (1)$$

Arterial p_{O_2} generally decreases with increasing exercise intensity and during constant-load high power exercise. For the general population such decreases are modest, while for trained athletes these decreases can be marked [3], [10]–[12]. For modeling purposes absolute declines of Δp_{O_2} = –2.5 to –15 mm Hg during phase 3 were considered, which represents a range from modest to severe decline [3], [10], [12]. A range of function types (e.g., third-order polynomial to simple linear) were also applied

to model $\Delta p_{O_2}(t)$ for phase 3, reflecting a range of forms that may be clinically encountered. An example third-order polynomial function is $p_{O_2}(t) = -0.0163t^3 + 0.233t^2 - 1.25t + 95.0$ for $\Delta p_{O_2} = -2.5$ mm Hg, where t is time in minutes. Subsequent research [8], reviewed in the following Section 4, solely applied exponential modeling since the exponential form more often reflects underlying biological processes and offers flexibility when extending to longer time periods. Note that modest declines in arterial p_{O_2} generally do not significantly affect percent hemoglobin saturation, in accordance with standard s-shaped dissociation curves [11].

T_{core} gradually increases in a linear or slightly concave-up manner during phase 3, and venous blood and rectal temperature increases of approximately 1°C are reported (or can be extrapolated from reported findings) [1], [3], [13]. Thus, within Simeoni & O'Reilly [7] T_{core} was linearly approximated by $T_{core}(t) = 0.185t + 37.0$, where t is again expressed in minutes.

Arterial p_{O_2} and T_{core} are the primary parameters of interest that vary within Eq. (1) for W, if $\dot{V}_{O_2}$ is set to a constant value of $\dot{V}_{O_2,SS}$. Hence, it was hypothesized that changes in W, resulting from changing p_{O_2} and T_{core} throughout phase 3, equate to the loss of efficiency depicted by the slow component of oxygen uptake and the subsequent need to increase $\dot{V}_{O_2}$ above $\dot{V}_{O_2,SS}$.

3.2 Results and Discussion for Slow Component Modeling

The increase in work from the onset of phase 3 required to compensate for described p_{O_2} decline and T_{core} increase is calculated from $-\Delta W$, as determined by Eq. (1), to give the model slow component $\dot{V}_{O_2}$ curves of Figure 4. When W per minute (i.e., power) is converted to equivalent $\dot{V}_{O_2}$ using the conversion 1 J ≡ 0.17 mL O_2, which is applicable to cycle ergometry work output, the model slow component curves closely align with curves obtained clinically [3], [6], [9]. The absolute changes in $\dot{V}_{O_2}$ for the model curves (0.08, 0.15, 0.30 and 0.43 L·min^{-1}) also agree with reported clinical values which range from 0.07 to 0.50 L·min^{-1} [2], [3], [6], [9]. When simple linear equations are used to model p_{O_2} variation, the model $\dot{V}_{O_2}$ curves also become linear (as shown for Δp_{O_2} = –2.5 mm Hg in Figure 4), highlighting the sensitivity of phase 3 towards this parameter and perhaps explaining why some reported clinical curves are also linear [2], [6]. Model curves are relatively less sensitive to T_{core} variation. Figure 4 demonstrates that the greater the decline in p_{O_2}, the greater the magnitude of the slow component, as expected from Eq. (1). This theoretical finding is consistent with the clinical finding that trained athletes are more likely to display relatively large slow components and declines in p_{O_2} (i.e., a hypoxic ventilatory response) during constant-load high power exercise, compared to untrained individuals [2], [10], [12].

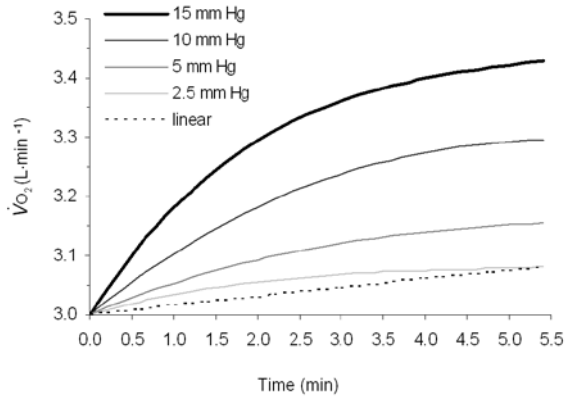

Figure 4. Modeled increase in $\dot{V}_{O_2}$ from the onset of phase 3 for Δp_{O_2} = –2.5, –5.0, –10 and –15 mm Hg. The dashed curve is for a linear model Δp_{O_2} = –2.5 mm Hg.

Simeoni and O'Reilly [7] summarized that the modeled increase in $\dot{V}_{O_2}$ throughout phase 3 approximates well the slow component of oxygen uptake kinetics, thus supporting the hypothesis from Eq. (1) that: decreases in W, resulting from decreasing p_{O_2} and increasing T_{core} throughout steady-state, constant-load high power exercise near the lactate threshold, equate to a loss of efficiency of the human body engine, giving rise to the slow component of oxygen uptake and the subsequent need to consume more fuel (O_2) to perform the same work.

4. Review of Endurance Event Modeling

This Section, reviewed from Simeoni [8], expands upon the thermodynamics-based model via its application to endurance sporting events to predict and explain observed race splitting strategies, subsequently demonstrating further model efficacy. The Section specifically considers steady-state oxygen uptake near the lactate threshold in an endurance swimming context. As per Section 3, the following primarily considers p_{O_2} decline and its effect on work output, and thus takes a relatively generic approach to endurance event energetics modeling.

It should be noted that the energetics of human activities and metabolism [14], [15] represent sophisticated fields of research (e.g., due to the complexity of adenosine triphosphate (ATP) synthesis mechanisms utilizing glucose and other sources), and so the generic approach adopted by this Section again represents a complementary perspective. Generally however, the energy determination for a given activity sees the total energy requirement shared between aerobic, anaerobic lactic acid and anaerobic alactic acid (associated with the depletion of phosphocreatine in working muscle) components, with energy distribution proportions dependent on both the type (each swimming stroke has its own mechanical efficiency) and level of physical activity. For swimming endurance events such as the 400, 800 and 1500 m freestyle, the above three energy components match the following approximate proportions [16]: 70, 25 and 5 % (400 m); 80, 20 and 0 % (800 m); 85, 15 and 0 % (1500 m).

4.1 Endurance Event Modeling Background

The concept of negative splitting a sporting race simply involves completing the second half of the race faster than the first half, with the aim of reducing fatigue and allowing a stronger finish to produce an optimal performance time. For swimming endurance events in particular, there is an expectation by many that a negative spilt strategy is applied by, and beneficial to, most athletes. However, in reality the percentages of male long course swimmers who negative split the 400, 800 and 1500 m freestyle events are respectively only about 14, 28 and 24%, based on a recent analysis of the top fifty men's times [17]. In fact for these events, Dobko shows that on average the first quarter of the race is fastest and the third quarter slowest (also second and fourth quarters are approximately at the same velocity but with the fourth marginally faster). In general, the described trend progressively flattens out with increasing race distance, and to various degrees the trend is also observed in women's swimming, as well as within athletics running events such as the 5000 and 10,000 m which often display a progressive gradual decline in running velocity with a final velocity surge or "kick" in the very last stage of the race.

The trend identified by Dobko [17] is partially reflected by the 2012 Olympic 1500 m freestyle final for men. When averaging the times of the eight finalists, the first half of the race is approximately 0.5 s shorter than the second half (i.e., a technically positive but approximately even split), with the gold medalist (world record) negatively splitting the event (by 1.26 s) largely due to a substantial burst in the last ≈250 m. The trend identified by Dobko [17] is certainly repeated by the 2012 Olympic 800 m freestyle final for women. When averaging the times of the eight 800 m finalists, the first half of the race is approximately 6 s shorter than the second half. The average split velocities for the aforementioned Olympic finals are displayed within Figure 5 (error bars represent ±1 SD), noticeably for which there is no distinct gradual trend upwards or approximate mid-way "step-up" in velocity.

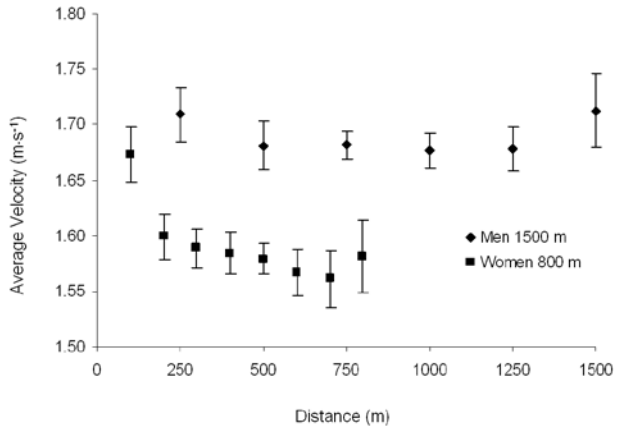

Figure 5. Average split velocities for 1500 m men and 800 m women freestyle 2012 Olympic finals. Error bars represent ±1 SD.

Thus, an apparent quandary exists between what is observed (where one may assume modern athletes functioning near the limit of human performance are applying ideal practical race strategies) and what is strongly endorsed (i.e., negative splitting) by many athletes and sports scientists of repute. Regardless of one's school-of-thought, all commentators would agree that commencing an endurance race at an excessively high velocity above the lactate (anaerobic/ventilatory) threshold would be unwise.

For the physical sciences readership, the lactate threshold corresponds to the maximum constant working intensity that can be sustained without the detrimental onset of blood lactate accumulation (above approximately 3 $mM \cdot L^{-1}$ for endurance trained athletes and 4 $mM \cdot L^{-1}$ more generally) which is exponential for graded exercise [18]–[20]. The lactate threshold also corresponds to the point at which $\dot{V}_{O_2}$ exceeds approximately 80 to 90% of the maximum oxygen uptake, $\dot{V}_{O_{2,max}}$ [20]. As raised in earlier Sections, the exact mechanisms of lactic acidosis-related fatigue and gradual increase from a steady-state $\dot{V}_{O_2}$ towards $\dot{V}_{O_{2,max}}$ (i.e., the slow component of oxygen update), observed during constant-load high power exercise near the lactate threshold, have captivated exercise physiologists for decades [2], [6] and for many the mechanisms still remain unclear. Indeed, at *submaximal* workloads whether lactate accumulation in muscle and blood is attributable to a hypoxic imbalance between oxygen supply and demand in the working muscles is controversial [21].

Ultimately, the splitting of a race for performance optimization involves integrating and minimizing lactic effects as a function of time and exercise intensity, balanced with the need to swim fast and minimize energy consumption, and practical outcomes following such considerations will dictate if a given splitting strategy is theoretically well designed. Optimization calculations, based simply on known energy costs of sporting events [14] that minimize performance time and energy expenditure have been performed (e.g., to predict optimal leg times for swim medley events) [22]. However, such calculations are not equipped to fully explain the earlier-identified trend for endurance events.

4.2 Results and Discussion for Endurance Event Modeling

In an ideal equilibrium mechanical situation, the Eq. (1) W for the "human body engine" under consideration is converted into the kinetic energy of locomotion (except for the at-rest metabolic energy requirement which equates to an oxygen uptake of approximately 0.25 $L \cdot min^{-1}$). Velocity can then be derived from a standard work-kinetic energy assignment, $v = \sqrt{2W/m}$, where m is athlete mass and W is based on $\dot{V}_{O_2}$ corrected via 0.25 $L \cdot min^{-1}$ subtraction and integrated over time. Naturally, velocity cannot increase indefinitely with W-time integration, lending to explanation of the equilibrium assignment whereby the aerobic work performed by the endurance swimmer equals the work performed by the water resistance to maintain approximate constant velocity.

Because the consideration of race splitting energetics represents the primary objective of this Section, rather than the prediction of absolute performance velocity, one may alternatively simply consider $v \approx k\sqrt{2W/m}$, where k is some constant of proportionality, for a more generic approach. However, the initial direct assignment will yield an interesting and justifiable outcome and so $k = 1$ is utilized for short-term analysis.

Figure 6 gives, for $m = 85$ kg, the resulting predicted velocity profile as a function of $\dot{V}_{O_2}$ for: (i) arterial $p_{O_2} = 105$ mm Hg, $T_{core} = 37\ ^{o}$C (approximate endurance event initial conditions), and (ii) arterial $p_{O_2} = 95$ mm Hg, $T_{core} = 38\ ^{o}$C (approximate endurance event steady-state example conditions). As suggested above, Figure 6 assumes an equilibrium condition with a $\dot{V}_{O_2}$ integration time of 1 s (i.e., work is based on per second volumetric values, vis-à-vis power).

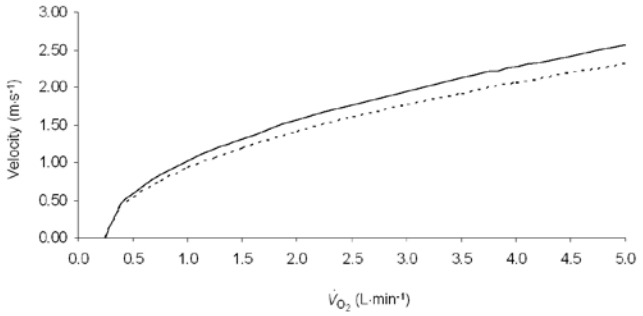

Figure 6. Predicted equilibrium velocity versus $\dot{V}_{O_2}$ (m=85 kg) for: arterial p_{O_2} = 105 mm Hg, T_{core} = 37 ^{o}C (—) and arterial p_{O_2} = 95 mm Hg, T_{core} = 38 ^{o}C (----).

From the dashed curve of Figure 6, $\dot{V}_{O_2,SS} \approx 3$ L·min^{-1}, representative of an endurance situation, corresponds to a predicted velocity of 1.76 m·s^{-1}. Additionally, from the averaging of the dashed and solid curves (for simple integration purposes to approximately represent a short duration "all-out" sprint rather than an endurance situation), $\dot{V}_{O_2,max} \approx 5\,\mathrm{L \cdot min^{-1}}$ corresponds to a predicted velocity of 2.44 m·s^{-1} (the latter approximation is included for interest only since the endurance situation remains the legitimate and primary focus of past and present studies). Interestingly, predicted velocities closely compare with average velocities of current men's swimming world freestyle records for endurance and sprint events respectively as per Table 1. The marathon 10 km average velocity (≈1.5 m·s^{-1}) aligns with an expectedly lesser $\dot{V}_{O_2}$.

Table 1. Predicted Equilibrium Velocities for Endurance and All-Out Conditions versus Men's World Long Course Swimming Freestyle Records.

Event	Velocity (m·s^{-1})	
	Model Predicted*	***World Record***
Endurance	1.76	1.72 (1500 m) 1.77 (800 m) 1.82 (400 m)
All-out	2.44	2.39 (50 m)

* m=85 kg applied; model $v \propto \sqrt{1/m}$.

The close agreement between predicted and average world record freestyle velocities is of interest and may provide further model efficacy in addition to that already provided by the accurate modeling of the slow component of oxygen uptake. Given that swimmers undoubtedly compete at the limit of human performance and Figure 6 is based on ideal work-energy transference in equilibrium, the likelihood of this further model efficacy should not be discounted. Of course, while such an optimized equilibrium assignment (upon which the v calculation is based) may either intuitively or from a physics perspective present as natural for freestyle swimming, the assignment does represent a simplification. The Appendix expands upon the physical basis of v modeling, and includes an integrated discussion of modeled power output.

To generalize Figure 6 for other aerobic-based sports one may rescale its y-axis (in accordance with $v \approx k\sqrt{2W/m}$) and Figure 7 indeed represents a relatively scaled version of the relevant endurance region of Figure 6, with accurate arterial $p_{O_2}(t)$ modeling also incorporated. As per Section 3, Δp_{O_2} can be modest (≈ –2.5 mm Hg), moderate (≈ –5.0 mm Hg), or severe (≈ –15 mm Hg) after 5 min of exercise, and $p_{O_2}(t)$ here is exponentially modeled as $p_{O_2}(t) = ae^{-bt} + c$, where t=0 corresponds to the onset of steady-state conditions near the lactate threshold. See Table 2 for model a, b and c parameters values. Figure 7 is for the moderate case of Δp_{O_2} = –5.0 mm Hg.

Table 2. Model Parameter Values for Arterial p_{O_2} Decline, of the form, $p_{O_2}(t) = ae^{-bt} + c$, During Steady-State Exercise near the Lactate Threshold.

Decline	Model Parameters*		
	a **(mm Hg)**	***b*** **(min^{-1})**	***c*** **(mm Hg)**
Modest	2.67	0.455	92.4
Moderate	15.3	0.102	80.0
Severe	26.0	0.170	70.0

* t=0 corresponds to the onset of stead-state conditions near the lactate threshold; model limit is t=6 min.

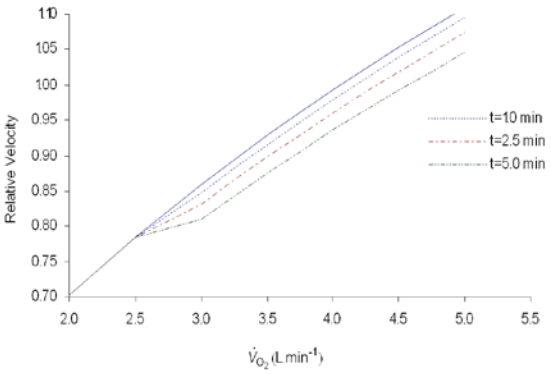

Figure 7. Theoretically achievable relative velocity for increasing exercise times of 1.0 to 5.0 min near and above the lactate threshold for moderate arterial $p_{O_2}(t)$ decline.

Returning to the primary Section objective of race splitting strategy analysis, Figure 7 demonstrates that as time progresses for a given $\dot{V}_{O_2}$ (fuel intake) the athlete (body engine) achieves progressively lower velocities, representing a progressive loss in engine efficiency reflected by ξ', where ξ' = achieved/ideal velocity. Analysis of Figure 7, together with similarly-constructed

graphs (not shown) for modest and severe arterial Δp_{O_2}, gives the following multivariable model equation for ξ':

$$\xi' = -0.0018 \cdot p_{O_{2,5}} \cdot t - 0.0010t + 1.00 \quad (2)$$

where $p_{O_{2,5}}$ is arterial p_{O_2} expressed in mm Hg after t = 5 min. The effect of $T_{core}(t) = 0.185t + 37.0$ modeling can also be incorporated within Eq. (2). However, the direct effects of in-isolation T_{core} changes are relatively less appreciable and left for Section 5 analysis and discussion.

Given the efficiency loss attributed to Eq. (2), the athlete can (i) increase effort and $\dot{V}_{O_2}$ to maintain velocity (risking the onset of lactate accumulation and lactic acidosis-related fatigue since the athlete is already near a limit of steady-state conditions), or (ii) maintain the same effort, resulting in a gradual and unavoidable decline in velocity due to efficiency decline. The modeled loss of efficiency for scenario (ii) is supported by the velocity decline observed during endurance events. For example, for a moderate $p_{O_{2,5}}$ decline of −4.5 mm Hg, Eq. (2) gives ξ' = 0.98 and 0.97 at t = 1.88 and 3.75 min respectively (approximate second and third quarter times for recent men's 800 m freestyle swimming world records), and these ξ' values closely correspond with those derived (ξ' = 0.980 and 0.975 respectively) from actual race velocities via second/first and third/first quarter velocity ratios. Although $p_{O_{2,5}}$ can to a limited degree be conveniently chosen, the highlighted ξ' agreement none-the-less again supports model efficacy.

Thus, it seems athletes may negative split endurance events even when race split times suggest otherwise. Viz., even if constant maximal steady-state effort is maintained, constant fuel consumption leads to a gradual decrease in velocity due to an unavoidable loss of "engine" efficiency. Any final stage surge would then result in an "effective" negative split, even if performance times suggest otherwise, due to the discussed progressive efficiency decline.

5. Temperature-Based Model Implications

5.1 Background to Temperature Dependency

It was noted in Section 3.1 that gradual T_{core} increases of approximately 1°C may occur during phase 3 of oxygen uptake kinetics [1], [3], [13]. It was also hypothesized from Eq. (1) that such T_{core} increases equate to a loss of "human body engine" efficiency because of the corresponding work output reduction. Although one might intuitively assume some efficiency reduction for such a thermally stressed engine, the influence of temperature on: the slow component of $\dot{V}_{O_2}$, exercise efficiency, and whole body metabolism generally, is surprisingly controversial or at least confounding [23]–[29]. For example, Koga *et al*. [24] find that elevated muscle temperature does not contribute to the slow component during heavy exercise, while MacDougall *et al*. [26] find slight but significant increases in $\dot{V}_{O_2}$ to be greater for hyperthermal conditions during heavy prolonged exercise. Similarly, Lee *et al*. [25] and Siegel *et al*. [29] find that ice slurry and cold drink ingestion decreases core body temperature and increases exercise endurance in the heat (findings of particular relevance towards the present article as discussed shortly), while Peiffer *et al*. [27] find that cold water immersion intervention does not improve 1 km cycling performance in the heat.

Recalling that $\dot{V}_{O_2}$ is dependent on a number of physiological variables and so any correlation or lack-thereof between $\dot{V}_{O_2}$ and T_{core} could potentially be confounded, the question raised by the above conflicting findings may therefore be summarized as: $\dot{V}_{O_2}$ and T_{core} may both change (typically increase) in a given exercise environment, but are T_{core} changes causal of any such $\dot{V}_{O_2}$ (and ultimately engine efficiency) changes, and, if so, what is the manner of any associated correlation?

Most researchers tend to agree that where $\dot{V}_{O_2}$ and corresponding T_{core} changes occur, the changes are *slight* [1], [3], [13], [24], [26], and this slightness is a likely contributing factor towards conflicting temperature-related research findings. Given the challenge of isolating temperature effects from the effects of more dominant factors (such as p_{O_2} changes noted previously), especially when an array of other competing secondary factors may exist (e.g., manner of induced heating/cooling, and the effect of variables in Eq. (1) such as ambient temperature), many quality studies that *appear* confounding are each expected to in fact be valid for their particular circumstances. The model application within the present Section, representing the final component of the encompassing and strategically concatenated explanation of the thermodynamics of exercise science, thus offers the potential advantage of allowing for quantitative assessment of subtle temperature effects in isolation, without interference from variables that otherwise compete clinically.

The present article is not considering, or suggesting model efficacy towards, seriously deleterious hyperthermia above approximately 40 °C where the human body's thermoregulatory system fails to cope and a significant decline in physical state results. Similarly, some contraindication of model efficacy is also expected when approaching a hyperthermic state.

5.2 Results and Discussion for Temperature Modeling

From Eq. (1), the work of the human body engine displays a linear relationship with V_{O_2} keeping all other variables constant. It follows that power output is also linear in $\dot{V}_{O_2}$ as displayed by Figure 8 for $\dot{V}_{O_2}$ = 2.5 to 3.0 L·min^{-1}.

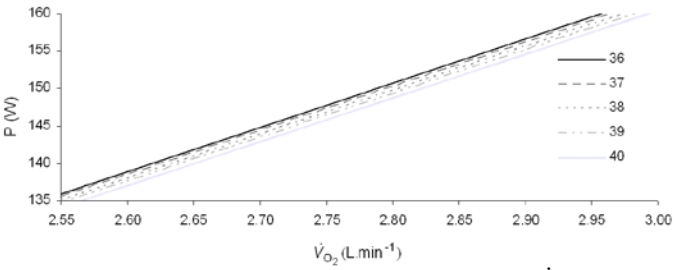

Figure 8. Power output predicted by Eq. (1) for $\dot{V}_{O_2}$ = 2.5 to 3.0 L·min^{-1} for T_{core} = 36, 37, 38, 39 and 40 °C. Other initial condition values held constant.

Figure 8 also displays the subtle temperature dependency of Eq. (1) via plots for T_{core} = 36, 37, 38, 39 and 40 °C, which in turn demonstrate an expected subtle inverse relationship between efficiency and temperature. All other variables in Eq. (1) are set to initial condition values as previously identified and the at-rest oxygen uptake rate is also inherently factored as per Section 4.

Engine efficiency as a function of T_{core} and relative to work output at T_{core} = 37 °C, $\xi_{T_{core}} = W_{T_{core}} \big/ W_{T_{core}=37.0\,^{o}\mathrm{C}}$, for a given $\dot{V}_{O_2}$ while maintaining other variables constant at initial condition values so as to isolate T_{core} effects, can similarly be derived from Eq. (1) and is given by the linear relationship of Eq. (3) and its corresponding Figure 9:

$$\xi_{T_{core}} = W_{T_{core}} \big/ W_{T_{core}=37.0\,^{o}\mathrm{C}} = -0.0032 T_{core}(t) + 1.119 \qquad (3)$$

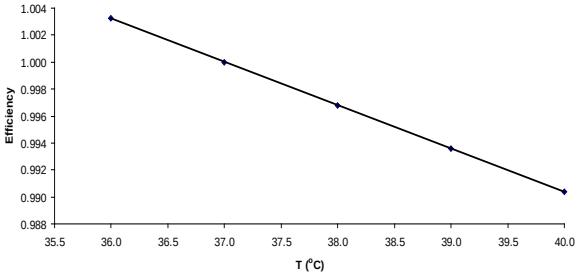

Figure 9. Human body engine efficiency, $\xi_{T_{core}}$, as a function of T_{core} in isolation.

Figure 9 displays a 0.32% efficiency decline per 1 °C increase in T_{core}, which translates to an approximate 0.5 sec per 1 °C increase disadvantage over a 5 min race (or event). For longer race durations involving heavy prolonged exercise where T_{core} increases of approximately 2 °C have been reported [26], the efficiency decline equates to an approximate 18 sec absolute disadvantage over a 90 min race. Assuming model validity, such disadvantages may with cursory glance appear minor, but of course within the context of high level competitive sporting events, such minor advantages/disadvantages have significant consequences and efficiency expectedly reduces further when other dependent model parameters effects are added to these in-isolation temperature effects (e.g., an endurance performance time degradation of ≈12% is predicted for ΔT_{core}= +2 °C and Δp_{O_2} = −15 mm Hg).

As outlined within Section 5.1, the subtleness of the $\xi(T_{core},t)$ functionality is in line with reported experimental observations. That is, it is difficult to compare theoretically predicted isolated $\xi(T_{core},t)$ impact findings and the ranging experimental findings of others because of the subtle nature of the quantified predictions and the in-practice confounding effects of variables such as p_{O_2} and ambient temperature, as per Eq. (1). However, it is the above subtleness, together with the generally expected loss of efficiency with increasing T_{core} for an engine under thermal stress, which provides further support for model efficacy. Assuming model validity, one can see from Eq. (1) why for example pre-event T_{core} cooling might bring slight performance improvement in one setting but no improvement in another (e.g., an ambient temperature decrease or increase in Eq. (1) can respectively counter or enhance some subtle improvement otherwise brought about by pre-event T_{core} cooling). Such sensitivity implications further support model efficacy since they provide some explanation for varied findings reported by others.

5.3 Rationalization of Cold Fluid Ingestion Effects on Endurance Exercise in the Heat

In apparent contrast to the somewhat subtle quantitative finding given by Eq. (3) and the subtle or null physiological research-based findings of others cited earlier [23], [24], [26], [28], are recent studies into the effects of ice slurry and cold drink ingestion on endurance exercise in the heat [25], [29]. These studies display remarkable findings such as: (i) a 19% increase in run time endurance for ice slurry versus cold water ingestion (with rectal temperature for the ice slurry protocol being 0.32 °C less than for the cold water protocol) [29]; and (ii) a 23% increase in cycling time endurance for cold versus warm water ingestion (with rectal temperature for the cold water protocol being 0.5 °C less than for the warm water protocol) [25]. The immediate question to be answered then is: how can such significant endurance time changes for such modest T_{core} changes reconcile with Eq. (3)? These remarkable cold fluid ingestion effects on endurance can in fact be rationalized with Eq. (3) by considering the human body's vascular and subsequent fluid dynamic responses to the ingestion as is discussed below.

5.3.1 Blood Temperature Response to Cold Fluid Ingestion

The blood's important circulatory heat distribution and dissipation role, e.g., for heat generated from biochemical oxidative reactions, is highlighted by the fact that blood temperature is higher than T_{core} by approximately 1 °C, and by the need for blood temperature control during hemodialysis to avoid considerable heat accumulation [30]. It is thus reasonable to consider the effect on blood temperature for the above aggressive cooling protocols that brought only modest T_{core} declines of 0.32 and 0.5 °C.

The temperature of the ice slurry mixture utilized by Siegel *et al.* [29] was −1 °C and the slurry was ingested over a 30 min period prior to exercise, with exercise commencing 5 min after ingestion completion. This aggressive cooling approach was facilitated by the fact that, in addition to the sub-zero temperature, ice-based cooling provides enhanced cooling (compared to cold water) because the latent heat of fusion for the ice-to-water phase change is largely absorbed from the body. Phase change-based cooling, for example involving application of an ice bag and wet ice, has been shown to significantly reduce subadipose tissue temperature at a depth of 1 cm as compared to non phase change-based cooling [31]. Subsequently, the aggressive ice slurry cooling of Siegel *et al.* [29] effectively brought about a prolonged T_{core} decline (after 30 min of exercise rectal temperature was still lower than that of the cold water ingestion protocol), but perhaps surprisingly only brought a relatively modest T_{core} decline of 0.32 °C.

During the 30 min of prolonged −1 °C ice slurry ingestion, significant localized conductive cooling takes place in the thoracic region and along the digestive tract. A significant cool sink (at lower than rectal temperature) exists, with blood circulatory heat redistribution taking place to eventually achieve thermal equilibrium. Hence, the modest T_{core} decline is accompanied by the fact that while

studies such as Siegel *et al*. [29] rigorously measure post-ingestion rectal and skin temperatures, arterial blood temperature will temporarily reduce below T_{core} in the circumstances described. Such reductions in arterial blood temperature partially reconcile with both Eq. (3) and the significant temperature effects reported by Siegel *et al*. [29] and similar studies.

Research into arterial (e.g., pulmonary) temperature fluctuations for ingestive cooling protocols is limited. However, the discussed blood cooling is mindful of the cold-stimulus headache brought on by ingesting cold foods too quickly [32] and the increase in blood pressure following the cold pressor test (hand immersion in ice water used as a cold sink) [33]. Even though the cold-stimulus headache, as well as more general cold-induced body pain and migraines (thought to be related) are all known to involve a significant and possibly primary neural mechanism, they are also known to involve a vascular mechanism involving arterial pulsation (e.g., significant blood cooling leading to constriction of sinus capillaries followed by a rapid progression from constriction to dilation as the blood again warms) [32]. Similarly, blood pressure increases (e.g., above 20/20 mm Hg) of the cold pressor test also have a vasoconstriction basis. To have such physical vascular effects, blood cooling following ingestive and/or cold sink cooling is clearly significant. Hence, while the formalism of the present article adopts a T_{core} nomenclature, Figure 3, together with the above discussion, enforce the fact that *arterial exchange* blood temperature at the capillary level is in fact the temperature of true model interest.

5.3.2 Vascular Response to Blood Temperature Decrease

Although the blood temperature response discussion of Subsection 5.3.1 partially reconciles Eq. (3) with the significant temperature effects reported by some [29], it does not fully reconcile, based on a conservative estimate of temporary blood temperature decline. This slight shortcoming now leads to further consideration of the vascular response to blood cooling following ice slurry or similar ingestion. It will be rationalized that the vascular response is accompanied by p_{O_2} increase, consistent with the known general finding of significant blood pressure increase after brief exposure to cold climate [34], due to vasoconstriction and an increase in effective blood viscosity.

Blood viscosity can increase by up to 300% as blood temperature decreases from 37 to 22 ^{o}C [35], [36], with viscosity increasing even more rapidly in the range 15 to 8 ^{o}C (this latter range is utilized during cardiac and thoracic aortic operations requiring deep hypothermia) [37]. Based on Poiseuille's law applicable to the small diameter microcirculation situation, a direct proportionality exists between driving pressure and viscosity (while maintaining a constant fluid flow rate). Thus, any significant blood temperature decrease is expected to bring about an effective blood viscosity increase, and subsequent p_{O_2} increase.

Furthermore, capillaries at the exchange level, where oxygen leaves the red blood cell and crosses the endothelium, have very small diameters of approximately 7.5 μm. Pries *et al*. [38] show that blood viscosity steeply increases for reducing tube diameter below ≈7 μm, and thus any cold-induced vasoconstriction at the relevant exchange level will again bring about blood viscosity and subsequent p_{O_2} increases[1]. Blood pressure increases of the cold pressor test can last up to two hours [39], and so such p_{O_2} increases could also have a meaningful lifetime. For auxiliary consideration, slight decreases in p_{CO_2} at the exchange level might also be considered and then would also contribute to the described effect.

To summarize, in addition to the direct positive effect of decreased temperature on work efficiency as governed by Eq. (3), a meaningful blood temperature reduction following prolonged ice slurry ingestion will also bring about a temporary blood viscosity increase due to both the viscosity's temperature dependency and capillary constriction. Such a viscosity increase will result in a meaningful p_{O_2} increase. The multiplicative effect of an increased efficiency as given by Eq. (3) and a dependent p_{O_2} increase in Eq. (1) would serve to amplify (via multiplicative enforcement) the resulting work increase, lending to explanation of the significant temperature effects reported by others [25], [29]. A similar rationale may be applied to explain cold versus warm water ingestion findings [25]. An approximate 18% improvement in endurance time is predicted by model combinations of p_{O_2} increase and T'_{core} decrease (with T'_{core} representing effective blood temperature at the exchange level) governed by the linear relationship, $\Delta p_{O_2} = 0.207\Delta T'_{core} + 19.3$.

5.3.3 Neurological Contributions to Cold Fluid Ingestion Effect

It should be noted that the positive "ice-slurry-type" effects on exercise endurance have, with a strong physiological basis, been attributed to a meaningful reduction in brain temperature that allows for more metabolic heat to be stored within the body core and limbs [29]. In addition, different degrees of thermoreception from receptors located in areas such as the mouth, esophagus and abdominal cavity, allowing the brain to perceive a lower-than-actual T_{core} (and thus "tricking" the brain), has also been postulated as a possible contributing mechanism for the positive effect cooling can have on exercise endurance [29]. The present article is intended as complementary. If reported physiologically meaningful brain temperature reductions associate with the temporary reduction in arterial blood temperature (at the capillary exchange level) discussed, then one can demonstrate further consistency between the presented physics- and cited physiology-based explanations, especially given that the hypothalamus (a heat regulating centre of the brain) is sensitive to blood temperature and accordingly controls vasoconstriction and dilation in response to blood temperature change.

6. Conclusions

The efficacy of the presented thermodynamics-based model, that considers the work associated with gas pressure, volume and temperature changes for the glucose-based equation of respiration, is supported by the model's:

[1] While the modeling of Pries *et al*. [38] offers a complete description, discussed increases can also largely be explained by the radius dependency within Poiseuille's law in which radius affects flow rate rather than viscosity, hence the use of the phrase "effective blood viscosity".

accurate modeling of the slow component of oxygen uptake; quantified explanation of observed race splitting strategies for endurance sporting events; accurate prediction of maximal velocities in swimming; and quantified explanation of temperature dependencies within oxygen uptake kinetics which in turn offers explanation of ranging temperature-related findings reported by others. The encompassing model thus contributes to the understanding and quantification of human oxygen uptake kinetics and the efficiency interdependencies of the human body engine.

Appendix: Swim Velocity Modeling and Considerations

Freestyle by its very nature is optimal but also unique in that it combines a highly efficient mechanical action with a near naturally buoyant situation, served by the fact that the average density of the human body is similar to (approximately 6% higher than) the density of water, and by the effective enhancement of buoyancy via the action of swimming itself. This optimal situation provides part basis for further explanation of the equilibrium condition upon which the *v* calculation of Section 4.2 is based.

The water resistance, or drag, force, F_D, acting against the swimmer is represented by the fundamental physics equation, $F_D = 0.5 C_D \rho v^2 A$, where C_D is a dimensionless scaling factor, ρ is water density, and A is the cross-sectional area of the swimmer. Reported values for C_D in an active swimming situation vary widely in the literature and the difficulty of measurement is acknowledged [40]. Based on the above fundamental equation and Newton's second law of motion the following governing differential equation can be written to model freestyle swimming:

$$P_S / v - 0.5 C_D \rho v^2 A = m dv / dt \tag{4}$$

where $P_S = \dot{W}$ is swimming power derived from the rate of Eq. (1), and assumes an optimal work-kinetic energy transference. Numerical solution of Eq. (4) (e.g., via Euler's method) is routine, and allows for example the modeling of *v* evolution at the start of the swimming race for an initial condition such as v_0 = 5.0 m·s^{-1} (typical starting block velocity), as represented by Figure 10.

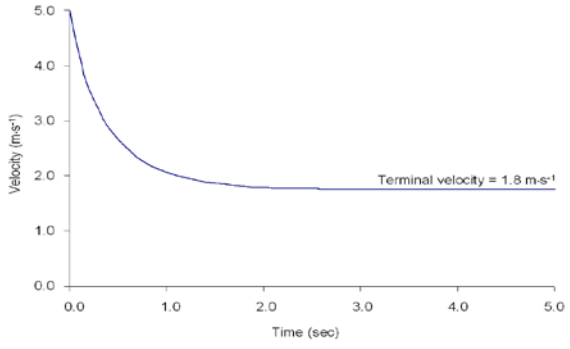

Figure 10. Numerical modeling of velocity evolution at the start of the swimming race (see text for model parameters).

Other model parameter values for Figure 10 include: P_S = 162 W corresponding to $\dot{V}_{O_{2,SS}} \approx 3$ L·min^{-1} with p_{O_2} = 105 mm Hg and T_{core} = 37 °C (i.e., before the onset of p_{O_2} decline and T_{core} increase); C_D = 1.0 [41]; ρ = 1000 kg·m^{-3}; A = 0.06 m^2; and dt = 0.1 s. The exponential decay from some relatively fast initial velocity, and realistic terminal velocity of v_T = 1.8 m·s^{-1}, in Figure 10 for stated typical parameter values, while not unexpected given earlier calculation, again brings support for model efficacy.

It is acknowledged that while reasonable values have been utilized, model parameters like C_D and A are known to be variable and difficult to measure in an active situation. However, their recognized uncertainties bring about opportunity since the model now allows for an exact statement of $C_D A$ product value for a known v_T. That is, from Eq. (4) the terminal condition, $C_D A = 2P_S / \rho v_T^3$, combines with Eq. (1) to give

$$C_D A = \left(p_{O_2} \cdot V_{O_2} \cdot T_{atm} / [T_{core} \cdot p_{CO_2}] - V_{O_2}\right) \cdot \left(p_{O_2} + p_{CO_2}\right) / 60 \rho v_T^3 \tag{5}$$

for per minute volumetric measurements. Potentially accurate $C_D A$ modeling by Eq. (5) can thus complement accurate F_D values measured by others, given that $F_D = 0.5 \rho v^2 (C_D A)$.

In terms of active C_D values cited by others, of interest is the finding of C_D values near 1.0 reported for fast teenage male and female freestyle swimmers up to the age of 16 years [41]. In that study C_D was shown to improve and approach 1.0 with increasing subject age and swimming proficiency (velocity). This finding raises the question: why is a "perfect" $C_D \approx 1.0$ result obtained for optimal freestyle swimming? Here, perfect is used in the sense of unity rather than minimization, since some geometric shapes possess $C_D < 1.0$. The answer to the afore-asked question is given below and supports the initial work-velocity assignment of Section 4.2.

The implication of $C_D \approx 1.0$ (leading to $F_D = 0.5 \rho v^2 A$) for a body of average density near, or effectively equal to, the density of its supporting fluid is that an analogous ideal fluid flow situation may be inferred. Ideal fluid flow which is non-turbulent is governed by the fundamental Bernoulli's equation (generally for swimming the more turbulent the fluid flow, e.g., via surface splashing, the greater the drag, and the swimmer aims for the smoothest possible flow). When approximately modeling the swimmer and surrounding water as simply two regions within such ideal flowing fluid, routine application of Bernoulli's equation for these two same-depth regions, one stationary and one flowing at *v*, then yields the pressure differential term of $\Delta P = F_D / A = 0.5 \rho v^2$ or $F_D = 0.5 \rho v^2 A$ as before. Substitution of the standard definition of ρ (mass/volume) reveals the expected kinetic energy underpinning of ΔP (expected since the $0.5 \rho v^2$ term of Bernoulli's equation is known as the kinetic energy term). Indeed, Eq. (4) is readily rearranged solely in terms of work and kinetic energy terms for $C_D = 1.0$. Hence, one again sees justification of the equilibrium work-velocity assignment of Section 4.2, where W is not only assumed to be optimally converted to kinetic energy, but also assumed to be in equilibrium with drag.

For the swimming endurance situation under investigation, the equilibrium drag force that corresponds to the power output predicted by Eq. (1) (and graphically displayed later by Figure 8) is of the order of 100 N, which is expectedly consistent with reported active drag force measurements for elite swimmers [42].

References

[1] J. M. Hagberg, J. O. Mullin, F. J. Nagle, Oxygen consumption during constant load exercise. *J. Appl. Physiol.: Respirat. Environ. Exercise Physiol., 45*, 381-384, 1978.

[2] D. J. Jacobsen, R. Coast, J. E. Donnelly, The effect of exercise intensity on the slow component of VO_2 in persons of different fitness levels. *J. Sports Med. Phys. Fitness, 38*, 124-131, 1998.

[3] D. C. Poole, W. Schaffartzik, D. R. Knight, T. Derion, B. Kennedy, H. J. Guy, R. Prediletto, P. D. Wagner, Contribution of excising legs to the slow component of oxygen uptake kinetics in humans. *J. Appl. Physiol., 71*, 1245-1260, 1991.

[4] B. J. Whipp, M. Mahler, *Pulmonary gas exchange vol. II*. New York: Academic, 1980.

[5] B. J. Whipp, S. A. Ward, N. Lamarra, J. A. Davis, K. Wasserman, Parameters of ventilatory and gas exchange dynamics during exercise. *J. Appl. Physiol., 52*, 1506-1513, 1982.

[6] J. A. Zoladz, B. Korzeniewski, Physiological background of the change point in VO_2 and the slow component of oxygen uptake kinetics. *J. Physiol. Pharm., 52*, 167-184, 2001.

[7] R. J. Simeoni, and J. O'Reilly, "A thermodynamics-based mechanism for the slow component of oxygen uptake kinetics during high power exercise," in *Proc. 16th National Congress, Australian Institute of Physics: Physics for the Nation*, Canberra, 2005.

[8] R. J. Simeoni, "Why athletes do not negative split some endurance events: A thermodynamics-based explanation," in *Proc. 5th International Conf. on Bioinformatics and Biomedical Engineering*, Wuhan, 2011.

[9] G. Camus, G. Atchou, J. C. Bruckner, D. Giezendanner, P. E. di Prampero, Slow upward drift of VO_2 during constant-load cycling in untrained subjects. *Eur. J. Appl. Physiol., 58*, 197-202, 1988.

[10] S. R. Hopkins, D. C. McKenzie, Hypoxic ventilatory response and arterial desaturation during heavy work. *J. Appl. Physiol., 67*, 1119-1124, 1989.

[11] S. K. Powers and E. T. Howley, *Exercise Physiology: Theory and Application to Fitness and Performance, 5th ed*. New York: McGraw-Hill, 2004.

[12] J. C. Richards, D. C. McKenzie, D. E. R. Warburton, J. D. Road, A. W. Sheel, Prevalence of exercise-induced arterial hypoxemia in healthy women. *Med. Sci. Sport. Ex., 36*, 1514-1521, 2004.

[13] R. Casaburi, T. W. Storer, I. Ben-Dov, K. Wasserman, Effect of endurance training on possible determinants of VO_2 during heavy exercise. *J. Appl. Physiol., 62*, 199-207, 1987.

[14] C. Capelli, D. R. Pendergast, B. Termin, Energetics of swimming at maximal speeds in humans. *Eur. J. Appl. Physiol., 78*, 385-393, 1998.

[15] C. E. K. Mady, S. Oliveira Junior, Human Body Energy Metabolism. *Int. J. Thermodynamics, 16*, 73-80, 2013.

[16] E. Maglischo, *Swimming fastest*. Champaign, IL: Human Kinetics, 2003.

[17] D. Dobko (Accessed 2010, Sept.). *How to split your open water swim* [Online]. Available: www.dobkanize.com.

[18] K. W. Borch, F. Ingjer, S. Larsen, S. E. Tomten, Rate of accumulation of blood lactate during graded exercise as a predictor of anaerobic threshold. *J. Sports Sci., 11*, 49-55, 1993.

[19] M. S. El-Sayed, K. P. George, D. Wilkinson, N. Mullan, R. Fenoglio, J. Flannigan, Fingertip and venous blood lactate concentration in response to graded treadmill exercise. *J. Sports Sci., 11*, 139-143, 1993.

[20] B. S. Rushall and F. S. Pyke, *Training for Sports and Fitness*, Hong Kong: MacMillan Education Australia, 1997.

[21] B. Grassi, V. Quaresima, C. Marconi, M. Ferrai, O. Cerretelli, Blood lactate and muscle deoxygenation during incremental exercise. *J. Appl. Physiol., 87*, 348-355, 1999.

[22] R. J. Simeoni, *Mathematics for Clinical Sciences 5th ed*. Gold Coast: Griffith University Press, 2002.

[23] M. J. Engelen, J. Porszasz, M. Riley, K. Wasserman, K. Maehara, T. J. Barstow, Effects of hypoxia on O2 uptake and heart rate kinetics during heavy exercise. *J. Appl. Physiol., 81*, 2500-2508, 1996.

[24] S. Koga, T. Shiojiri, N. Kondo, T. J. Barstow, Effect of increased muscle temperature on oxygen uptake kinetics during exercise. *J. Appl. Physiol. 83*, 1333-1338, 1997.

[25] J. K. Lee, S. M. Shirreffs, R. J. Maughan, Cold drink ingestion improves exercise endurance capacity in the heat. *Med. Sci. Sport. Ex., 40*, 1637-1644, 2008.

[26] J. D. MacDougall, W. G. Reddan, C. R. Layton, J. A. Dempsey, Effects of metabolic hyperthermia on performance during heavy prolonged exercise. *J. Appl. Physiol., 36*, 538-544, 1974.

[27] J. J. Peiffer, C. R. Abbiss, G. Watson, K. Nosaka, P. B. Laursen, Effect of cold water immersion on repeated 1 km cycling performance in the heat. *Med. Sci. Sport. Ex., 13*, 112-116, 2010.

[28] L. B. Rowell, Human cardiovascular adjustments to exercise and thermal stress. *Physiol. Rev., 54*, 75-159, 1974.

[29] R. Siegel, J. Mate, M. B. Brearley, G. Watson, K. Nosaka, P. B. Laursen, Ice slurry ingestion increases core temperature capacity and running time in the heat. Med. *Sci. Sport. Ex., 42*, 717-725, 2010.

[30] D. Schneditz, C. Ronco, N. Levin, Temperature control by the blood temperature monitor. *Semin. Dial., 16*, 477-482, 2003.

[31] M. M. Merrick, L. S. Jutte, M. E. Smith, Cold modalities with different thermodynamic properties produce different surface and intramuscular temperatures. *J. Athl. Train., 38*, 28-33, 2003.

[32] J. Hulihan, Ice cream headache. *British Medical Journal, 314*, 1364, 1997.

[33] M. A. Greene, A. J. Boltax, G. A. Lustig, E. Rogow, Circularly dynamics during the cold pressor test. *American J. Cardiology, 16*, 54-60, 1965.

[34] Z. Sun, X. Wang, C. E. Wood, J. Robert Cade, Neurohumoral control of cardiovascular function. *American Journal of Physiology: Regulatory, integrative and Comparative Physiology, 288*, R433-R439, 2005.

[35] P. W. Rand, E. Lacombe, H. E. Hunt, W. H. Austin, Viscosity of normal human blood under normothermic and hypothermic conditions. *J. Appl. Physiol., 19*, 117-122, 1964.

[36] A. Reis, N. Kirmaier, The viscosity-temperature function of blood and its physio-chemical information content. *Biorheolohy, 13*, 143-148, 1976.

[37] D. M. Eckmann, S. Bowers, M. Stecker, A. T. Cheung, Hematocrit, volume expander, temperature, and shear rate effects on blood viscosity. *Anesth. Analg., 91*, 539-545, 2000.

[38] A. R. Pries, D. Neuhaus, P. Gaehtgens, Blood viscosity in tube flow: dependence on diameter and hematocrit. *Am. J. Physiol., 263* (*Heart Circ. Physiol.* 32), H1770-H1778, 1992.

[39] Z. Sun, Cold weather hikes blood pressure, UF Scientist warns, *Science Daily*, University of Florida Health Science Centre, Feb. 2005.

[40] R. Havriluk, Variability in measurement of swimming forces: A meta-analysis of passive and active drag. *Research Quart. Exercise Sport, 78*, 32-39, 2007.

[41] R. Havriluk, "Performance level differences in swimming drag coefficient," in *Proc. 7th IOC Olympic World Congress on Sport Sciences*, Athens, 2003.

[42] Swimright (Accessed 2013, April 11). The physics and biomechanics of swimming [Online]. Available: www.swimright23.webs.com/dragresistance.htm.